MICROMECHANICAL ASPECTS OF TRANSGRANULAR AND INTERGRANULAR FAILURE COMPETITION

I. DLOUHÝ [a]) AND O. NĚMEC [b]),

[a]) *Institute of Physics of Materials, Academy of Sciences of the Czech Republic, 61662 Brno*
[b]) *Department of Materials Engineering, Technical University of Ostrava, 70833 Ostrava, Czech Republic*

ABSTRACT

Main purpose of the work was to quantify causes and characteristics governing the intergranular fracture initiation and occurrence of this fracture micromechanism in competition with cleavage one. A CrNi steel of commercial quality and the same steel with increased content of impurity elements have been used for investigation. Step cooling treatment has been applied in order to induce intergranular embrittlement and brittle fracture initiation in both steel melts. Except for standard specimen geometry for three-point bending the pre-cracked Charpy type specimens were applied for determination of fracture mechanical properties. Fractal analysis was applied in order to characterise the quantitative morphological differences in fracture surfaces. Relation of cleavage fracture stress and critical stress for intergranular failure has been followed.

KEYWORDS

Brittle fracture initiation, cleavage, intergranular failure, impurities effect, fracture toughness

INTRODUCTION

Recent procedures of metal metallurgy standardly produce alloys with relatively high purity. For the, commonly used materials, the key problem to be answered is how to determine a criterion for effective determination of acceptable impurities level in metal/steel taking into account its operational properties instead of further escalation of metal purity [1,2]. In many applications such a criterion seems to be more susceptible than direct impurity content determination. In case of brittle failures the role of impurities have to be seen in assistance in embrittling processes taking place in microstructure during some welding a tempering procedures (technological degradation) or during some thermal exposition (operational degradation) [3,4].

In embrittlement of technological nature - heat affected zones, overheated microstructures etc. - impurities atoms are attracted to grain boundaries causing their weakening [5]. Usually, these changes are associated with intergranular fracture micromechanism as result of embrittlement. In weld metal very specific role of inclusion in cleavage fracture is often assessed as the inclusion triggered cleavage may strongly overlap an inherent metal toughness in many cases [6,7].

In embrittlement due to long term thermal exposition two micromechanisms control the changes in fracture micromechanism: (i) temper embrittlement caused by growth of carbide

diameter leading to change of transgranular cleavage from dislocation triggered to carbide induced [9]. (ii) intergranular embrittlement caused by contemporary effect of diffusion of impurities and carbide coarsening at grain boundaries and/or interface boundaries [2,3 etc.].

It is obvious that occurrence of intergranular initiation could be taken as significant simple measure of limit specifying the negative influence of impurities content. This micromechanism type was usually responsible for strong decrease of mechanical properties [8,9 etc.], anomalous fracture behaviour or, at least, comparably larger and unacceptable data scatter.

The intergranular fracture initiation has to be taken as result of competition between two stress-controlled fracture micromechanisms: cleavage and intergranular. For both micromechanisms action a condition of local fracture stress acting over some microstructurally susceptible distance has to be filled. What is the cause that forces the metal grain boundary to fail in intergranular manner rather than transgranular? As generally known, it is one of major physical quantities, cohesion strength, that decrease at the same time as the cleavage fracture stress is kept on the same level. But there is lot of questions connected with relation of microscopic cohesion strength and local fracture stress, with effect of pre-strain due to cold deformation or constraint phenomena etc. An interconnection of fractographic methods with sophisticated analysis of data from Charpy type specimen (or other simple suitable specimen) seems to be effective and key tool for assessment of (negative) effects of impurities, inclusion and other metallurgy effects.

The aim of paper can be seen in analysis of micromechanical aspects of brittle fracture initiation connected with intergranular decohesion as micromechanism that is well susceptible to metallurgic cleanliness and cumulative degradation of material. Causes and characteristics governing the intergranular fracture initiation and occurrence of this fracture micromechanism in competition with cleavage one should be also addressed.

MATERIAL AND EXPERIMENTAL PROCEDURES

Material characteristics
Two different melts of CrNi pressure vessel steel have been used having the chemical composition shown in table 1.

Table 1. Chemical compositions of steel melts used in investigation (in wt %)

Melt designation	C	Mn	Si	Cr	Ni	S	P	Sn	Sb	As
A (as received)	0,15	0,40	0,21	0,72	3,51	0,011	0,010	0,003	0,005	0,002
R (remelted)	0,20	0,45	0,145	0,74	3,57	0,013	0,011	0,014	0,036	0,005

The steel melt A has been received as commercially produced hot rolled bar having section 80x80 mm^2. The impurities content in this steel was qualified as common. The steel melt R has been prepared from the as received melt A by remelting in induction furnace adding Sn and Sb (table 1).

The following microstructures have been prepared for investigation in both these steel melts: (i) standard (ferritic) microstructure (state obtained by normalisation treatment from 940 °C with quenching into water and tempering for about 100 h at 650 °C), and (ii) ferritic microstructure in embrittled conditions (the same microstructure as in case (i) additionally

thermally aged). The embrittling ageing applied was either isothermal (IA) at 550°C for 150 h or so called step-cooling regime (SC – as shown in work [10]).

Selected materials characteristics are shown in Table 2. In this table, the value of d_F represents ferritic grain size. Basic mechanical properties shown here were obtained at room temperature. Fracture appearance transition temperature (FATT) has been introduced here as characteristics describing the location of transition region on temperature axis of all for steel microstructures.

Table 2. Microstructural and selected mechanical characteristics of materials studied

Micro-structure	tempering	d_F [μm]	$R_p0.2$ [MPa]	R_m [MPa]	CVN imp. energy [J]	FATT [°C]
A/	initial state	16	490	621	260	-80
A/ IA	isothermal	18	510	658	210	-75
A/ SC	step cooling	17	508	652	205	-60
R/	reference state	17	485	605	156	-40
R/ SC	step cooling	19	496	632	85	+25

Mechanical testing

The yield strength and other tensile properties including true stress-strain curves have been measured using cylindrical specimens with diameter of 6 mm and gauge length 25 mm being loaded over temperature range of -196 to +200 °C at the cross-head speed of 2 $mm.min^{-1}$.

For steel melt A the temperature dependencies of fracture toughness have been measured using 25 mm thick specimen loaded in three point bending at the cross-head speed of 1 $mm.min^{-1}$. Standard procedures have been applied for fracture toughness determination. For both steel melts, A and R, pre-cracked Charpy type specimens have been also applied for the fracture toughness tests because of limited amount of experimental material of steel R. The standard fracture toughness temperature diagrams have been evaluated by means of master curve methodology [11].

Temperature dependencies of CVN impact energy were measured statically and dynamically. Fracture appearance transition temperatures (FATT) have been determined among others. To evaluate the local fracture stress, σ_f, the load - displacement traces have been recorded, and the maximum force, fracture force, and general yield force, respectively have been taken from records and plotted against temperature. For one selected temperature below t_{gy}, temperature where fracture and general yield force were coincident, a range of bend tests was performed to obtain data for statistical treatment for all microstructures tested. The detailed analysis is available in [10].

Fractography and supporting procedures

For CVN specimens tested around and below the brittleness transition temperature, t_{gy}, the distances of the fracture initiation sites from the notch root were evaluated using SEM micrographs. To identify the microstructural causes of cleavage facet nucleation the triggering origins of facets in failure initiation sites were assessed. Similar procedures were applied in order to prove the correlation of intergranular facets with ferritic grain size.

Fractal dimension analysis has been applied in order to characterise the fracture surfaces quantitatively. The method principles have been in detail described elsewhere [12]. The value of fractal dimension, D_F, has been determined from metallographic sections perpendicular to

fracture in direction of crack propagation. Dependences of D_F on distance from the crack tip has been analysed in mentioned publication, the mean value corresponding to brittle fracture morphology was used for purposes of this work.

For test temperature below general yield temperature, t_{gy}, (see table 3) the principal stress distributions below the notch were calculated. A 3D approach was developed for the elastic-plastic analysis. Standard finite element computer code ABAQUS was used for these purposes.

RESULTS AND DISCUSSION

Fracture behaviour of the steel

The typical temperature dependence of fracture toughness is shown in Fig. 1 for the steel A in initial state. In order to determine the scatter band of fracture toughness values in the transition and lower shelf regime a number of specimens was tested at one temperature and data obtained are also given in the figure. For purposes of comparison with other microstructural states investigated the validity of master curve methodology was proved. The master curve is represented by full line; the 90 % probability scatter band is shown by dashed curves. The transition from cleavage to ductile fracture initiation is represented in figure by temperature t_{DBL} . The ductile tearing preceding the cleavage was determined fractographically and has been indicated by symbols K_{Ju} and K_{Jm} in figure.

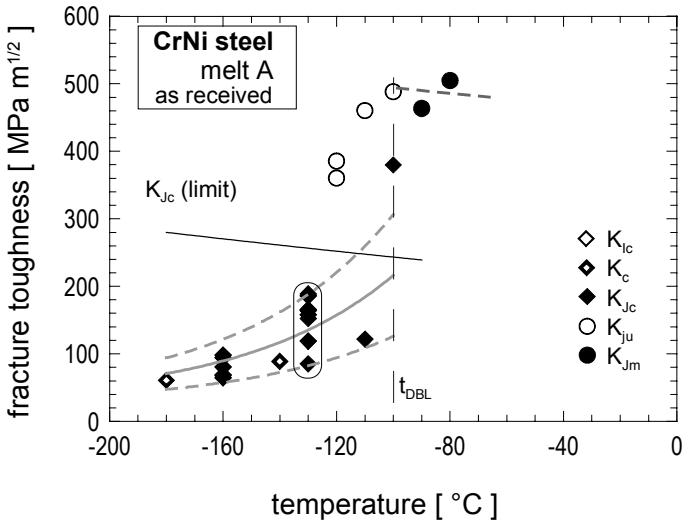

Fig. 1. Fracture toughness temperature diagram for the steel with initial microstructure

The following Fig. 2 shows the fracture properties for steel A and R after step-cooling treatment (represented by scatter band limited by dashed and full lines respectively). The as received state is here represented by thin dashed lines only. It follows from comparison of main trends that except for the scatter in fracture toughness values a very limited embrittlement occurred and only slight shift of transition region was observed for melt A.

No extensive intergranular fracture was identified in fracture surfaces as shown in Fig. 3a. Almost transgranular cleavage can be seen in fracture surfaces. Some grain boundaries embrittlement occurred however; the evidences can be seen in secondary microcracks oriented perpendicularly to major crack and usually in triple points of initial grain boundaries.

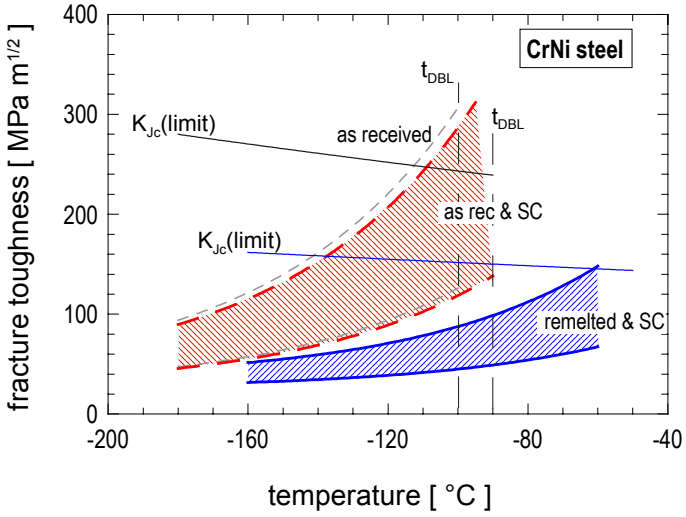

Fig. 2. Comparison of FTTD for both steel melts after and step cooling treatment

It follows from the figures 2 and 3a that it is practically impossible to produce by applied ageing procedures more extensive (intergranular) embrittlement in steel A (with fine-grained microstructure). The change in fracture toughness and fracture behaviour is practically so low, that no remarkable embrittlement occurs.

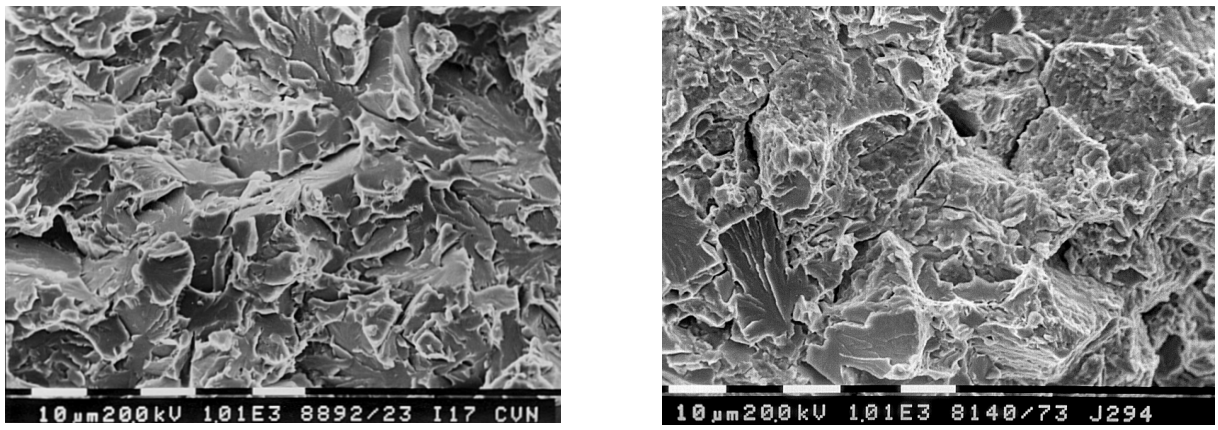

Fig. 3. Examples of fracture surface in lower shelf region after step cooling treatment
a) left side melt A; b) right side melt R

For melt R after step cooling treatment the fracture appearance of pre-cracked specimen tested in lower shelf region is obvious from Fig. 3b. More than 60 % of intergranular fracture was observed. In connection with the shift of transition region to much higher temperatures, with the shift of transition for CVN impact energy [10] - (see also the FATT in table 2) and with the significant decrease of fracture toughness in lower shelf and transition region the detrimental impurity content at grain boundaries is clearly obvious.

Quantitave characterisation of fracture surfaces

Several experimental approaches of fractal dimension determining were followed extensively in order to generate the representative quantification of the fracture morphology [12]. The metallographic sections perpendicular to fracture plane in direction of crack propagation has been found as the most representative. For calculation of fractal dimension the Richardson's formula has been applied having after the mathematical derivation the following form:

$$D_F = 1 - \frac{d \log R_L}{d \log \eta} ,$$

where R_L is the roughness parameter of fracture profile, R_{L0} is a constant, η is the length of the yardstick and D_F is fractal dimension. The fractal dimension was acquired from the empirical measurement of the fracture profile as the slope of a linear regression dependence $logR_L$ vs $log\eta$. The length size of the yardstick depends on proportions of characteristic units, out of which the fracture surface is composed. The smallest length of yardstick was η=3.4μm.

The Fig. 4 shows part of results. First of all, the separate values represent data obtained for steel A in initial state and in embrittled state. Except for separate data the scatter bands are shown for initial state represented by full lines only, for the state after embrittling ageing by shaded field. It follows from comparison that practically the same values of fractal dimension seems to be the main characteristics of brittle failure for both microstructures - initial and embrittled. Based on this finding and based on knowledge shown in previous part, the "embrittled" state of steel A posses still acceptable properties and embrittlement process is just in stage of conversion to intergranular initiation. On the other side evident differences have been found when comparing both embrittled microstructures of the steel melt A and R (compare the both shaded fields), the higher value of fractal dimension corresponds to higher fracture roughness due to intergranular failure mechanism (for comparisons see also the values of D_F shown in Table 3).

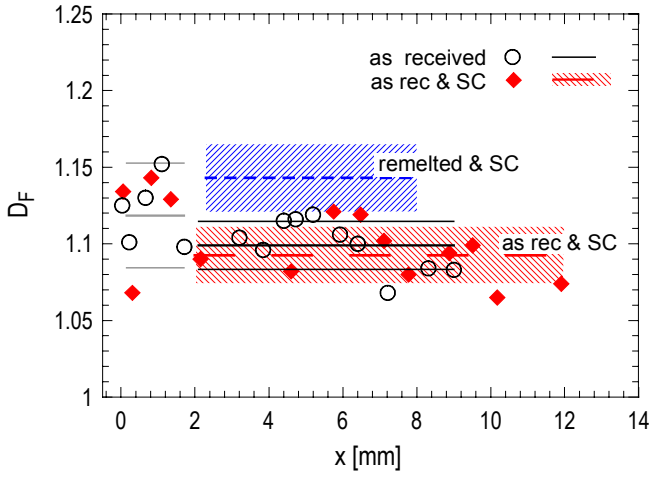

Fig. 4. Change of fractal dimension, D_F, with distance from crack tip, x, – steel A with initial microstructure and after ageing, steel R after step cooling

Table 3. CVN specimens, local fracture stresses σ_f and characteristics of fractal dimension D_F

steel melt	State	t_{gy} [°C]	σ_f [MPa]	failure micromechanism in brittle initiation origin	D_F	standard deviation
A-as rec	Initial	-140	2472	cleavage	1.099	0.015
	embrittled by IA	-160	2185	cleavage – intergranular	1.093	0.018
	embrittled by SC	-120	2121	cleavage – intergranular		
R-remelted	initial reference	-145	2216	cleavage		
	embrittled by SC	-65	1791	intergranular	1.143	0.031

Critical (fracture) stress quantification
To determine the local fracture stress experimentally two procedures were used:

(i) For CVN specimens loaded statically or dynamically, at temperatures where the fracture and general yield forces were coincident, the local maximum tensile stress was calculated taking the value of 2,24 of plastic stress concentration factor $k_{\sigma p}$. The relation of measured static and dynamic yield strength and general yield forces has been determined. The simplified approach was used for calculation of local fracture stress σ_f from general yield force, applying the equation $\sigma_f = 106.\ F_{gy}$.

(ii) For a range of CVN specimens tested statically in bending at one temperature tensile stress distributions below the V notch were calculated using FEM. The distances between the initiation origin and the notch root were measured from SEM micrographs. The distances were applied into calculated maximum tensile stress distributions and local stress corresponding to fracture was read. The results obtained were compared with procedure (i) with good correlation.

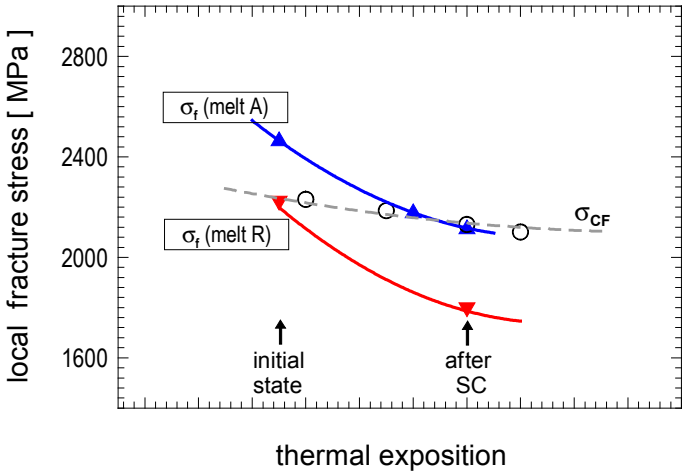

Fig. 5. Effect of embrittling thermal exposition on critical fracture stress

Comparison of local fracture stress values (σ_f) obtained for both steel melts and microstructures tested is shown Fig. 5. This figure shows the relationships between the cleavage fracture stress, σ_{CF}, controlling failure in un-embrittled microstructures and critical fracture stress, σ_C, controlling failure in embrittled microstructures. Both characteristics are here schematically plotted (full curves) into dependence on thermal exposition. As thermal exposition arbitrary quantity could be applied characterising either cumulative exposition on temperatures (through tempering parameter etc.) or the chemical changes on grain boundaries

(impurities atom enrichment etc.). A curve representing the change in cleavage fracture stress with tempering (without attracting impurity atoms to grain boundaries) is shown here. In case the local fracture stress σ_f is above this curve the fracture could tend to be transgranular cleavage ($\sigma_C > \sigma_{CF}$), below this curve intergranular ($\sigma_C < \sigma_{CF}$).

From the change in critical stress corresponding to thermal exposition (ageing or step cooling) is evident that in steel with higher purity the local fracture stresses are comparably higher than for lower quality steel. For steel with good cleanliness (the upper full curve) the relatively high values σ_f have been determined for initial state but also for conditions after embrittling treatment. Under the conditions of comparably strong impurity enrichment of grain boundaries, the fracture is still controlled by cleavage rather than by intergranular decohesion. For steel with poor cleanliness two positions are characteristic for the change of local fracture stress σ_f (lower full curve). The upper value of σ_f corresponds more to cleavage (σ_{CF}) the lower value more to intergranular fracture (σ_C).

CONCLUSIONS

Causes and characteristics governing the intergranular fracture initiation and occurrence of this fracture micromechanism in competition with cleavage one have been quantified in this work. It has been found that the (local) fracture stress is lower for steel with intergranular initiation when compared to the steel with pure cleavage failure mechanism. Fractal dimension corresponded well to brittle fracture mophology reflecting, on quite susceptible level, the changes from pure cleave to intergranular fracture. From this observations follow that the fracture stress may be used as local criterion of fracture and as one of parameters for identification of critical impurity levels causing intergranular embrittlement.

ACKNOWLEDGEMENTS

Authors gratefully acknowledge to Ministry of Education, Youth and Sport (contract Nr. OC 517.20) and to Grant agency of the Academy of Sciences (A2041003) for their financial support.

REFERENCES

[1] J. Nutting: Ironmaking and Steelmaking, 1989, 16, No. 4, p. 219.
[2] C. L. Briant, S.K. Banerji: Int. Metals Review, 1978, 23, p. 164.
[3] J. Kameda: Acta Metall, 1986, 34, p. 867.
[4] M. Holzmann, J. Man, B. Vlach & J. Krumpos: *Int. J. Pres. Ves. and Piping* , 1994, 57, 141.
[5] J. Pokluda, P. Šandera, J. Zeman: ASTM - STP 1131, 1992, p. 653.
[6] S.T. Mandziej: Scripta Met. & Mat., 1992, 27, p. 793.
[7] I. Dlouhý, V. Kozák, L. Válka, M. Holzmann: J. de Physique IV, C6 - 205.
[8] J. Man, M. Holzmann, B. Vlach: Zváranie (Welding) 1983, 32, p. 3.
[9] M. Holzmann, I. Dlouhý, B. Vlach & J. Krumpos: Int. J. Pres. Ves. and Piping, 68, 1996, 99.
[10] I. Dlouhý, L. Válka, J. Pokluda: COST Workhsop, 1999, Řež
[11] ASTM, E1921-97, 1997, Standard Test Method For the Determination of Reference Temperature T_0 for Ferritic Steels in the Transition Range.
[12] O. Němec, M. Holzmann, I. Dlouhý, Fraktography 2000, Stará Lesná, p. 116.